AD_____

Award Number: DAMD17-02-1-0440

TITLE: Novel Image Analysis to Link Sub-Nuclear Distribution of Proteins with Cell Phenotype in Mammary Cancer

PRINCIPAL INVESTIGATOR: David W. Knowles, Ph.D.

CONTRACTING ORGANIZATION: Ernest Orlando Lawrence Berkeley National Laboratory
Berkeley, CA 94720

REPORT DATE: May 2003

TYPE OF REPORT: Annual

PREPARED FOR: U.S. Army Medical Research and Materiel Command
Fort Detrick, Maryland 21702-5012

REPORT DOCUMENTATION PAGE

Form Approved
OMB No. 074-0188

1. AGENCY USE ONLY (Leave blank)	2. REPORT DATE	3. REPORT TYPE AND DATES COVERED
	May 2003	Annual (23 Apr 2002 - 22 Apr 2003)

4. TITLE AND SUBTITLE
Novel Image Analysis to Link Sub-Nuclear Distribution of Proteins with Cell Phenotype in Mammary Cancer

5. FUNDING NUMBERS
DAMD17-02-1-0440

6. AUTHOR(S)
David W. Knowles, Ph.D.

7. PERFORMING ORGANIZATION NAME(S) AND ADDRESS(ES)
Ernest Orlando Lawrence Berkeley National Laboratory
Berkeley, CA 94720

E-Mail: dwknowles@lbl.gov

8. PERFORMING ORGANIZATION REPORT NUMBER

9. SPONSORING / MONITORING AGENCY NAME(S) AND ADDRESS(ES)
U.S. Army Medical Research and Materiel Command
Fort Detrick, Maryland 21702-5012

10. SPONSORING / MONITORING AGENCY REPORT NUMBER

11. SUPPLEMENTARY NOTES
Original contains color plates: All DTIC reproductions will be in black and white.

12a. DISTRIBUTION / AVAILABILITY STATEMENT
Approved for Public Release; Distribution Unlimited

12b. DISTRIBUTION CODE

13. ABSTRACT (Maximum 200 Words)
The goal of this project is to develop novel optical imaging/image analysis techniques that will allow automated, quantitative screening to distinguish malignant, pre-malignant, and non-malignant mammary tissue. Our hypothesis is that cellular and tissue phenotype is reflected by the organization of components within the nucleus. The past year has produced positive results regarding the use of the quantitative imaging and analysis to relate difference in the distribution and organization of nuclear mitotic apparatus protein to the phenotype of nonmalignant and malignant cell populations in the proliferative, early growth stage. The development of a new mage analysis technique shows clear differences in the organization of NuMA foci between nonmalignant proliferating cells and malignant proliferating cells. By extending our studies into normal and malignant human tissue we report that the NuMA organization in differentiated nonmalignant cell of our tissue model system has a normal phenotype. Further, we believe that refinements to our new analysis technique will reveal at least two population existing in our images of malignant human tissue. By quantifying the spatial distribution of these proteins in this relevant culture model system, the work is providing understanding of how such distributions correspond with the phenotype of the cells.

14. SUBJECT TERMS
Breast cancer, NuMA, Quantitative Imaging

15. NUMBER OF PAGES
17

16. PRICE CODE

17. SECURITY CLASSIFICATION OF REPORT	18. SECURITY CLASSIFICATION OF THIS PAGE	19. SECURITY CLASSIFICATION OF ABSTRACT	20. LIMITATION OF ABSTRACT
Unclassified	Unclassified	Unclassified	Unlimited

Table of Contents

Annual Report May 2003

Novel Image Analysis to Link Sub-Nuclear Distribution of Proteins with Cell Phenotype in Mammary Cancer

Investigator: David Knowles (Collaborating laboratories: Sudar, Lelièvre, Bissell)

INTRODUCTION:

The goal of this project is to develop novel optical imaging / image analysis techniques that will allow automated, quantitative screening to distinguish malignant, pre-malignant, and non-malignant mammary tissue. Our hypothesis is that cellular and tissue phenotype is reflected by the organization of components within the nucleus. The past year has produced positive results regarding the use of the quantitative imaging and analysis to relate difference in the distribution and organization of nuclear mitotic apparatus protein to the phenotype of nonmalignant and malignant cell populations in the proliferative, early growth stage. The development of a new image analysis technique shows clear differences in the organization of NuMA foci between nonmalignant proliferating cells and malignant proliferating cells. By extending our studies into normal and malignant human tissue we report that the NuMA organization in differentiated nonmalignant cell of our tissue model system has a normal phenotype. Further, we believe that refinements to our new analysis technique will reveal at least two population existing in our images of malignant human tissue. By quantifying the spatial distribution of these proteins in this relevant culture model system, the work is providing understanding of how such distributions correspond with the phenotype of the cells.

BODY:

In the first year of work (Months 1 - 12) we have focused on the distribution nuclear mitotic apparatus protein, NuMA in a progression series of cultured HMT-3522 human mammary epithelial cells (HMECs) that mimic early stages of cancer development. Non-malignant S1 HMT-3522 cells recapitulate differentiation into phenotypically normal breast glandular structures in 10 day of three-dimensional (3D) culture. 3D culture is preformed by placing cells in contact with an exogenous extracellular matrix enriched in basement membrane components (Matrigel), and supplying cells with essential growth factors and hormones. Glandular structure formation encompasses cell proliferation (until day 6), growth-arrest and deposition of a continuous endogenous basement membrane around the glandular structure. Malignant T4-2 HMT-3522 cells mimic tumor growth, with the formation of disorganized multicellular structures in which cells keep proliferating, when cultured in the same conditions. NuMA has been previously found to undergo remarkable changes in its nuclear organization during glandular structure formation (Lelièvre et al., 1998). During the proliferating stage the distribution patterns of NuMA appear homogenous throughout the cell nucleus and was seem similar to what is observed in tumor cells. Whereas, upon differentiation, NuMA is reorganized into a ring-like pattern at the periphery of the cell nucleus. Culturing of the cells and fluorescence labeling of the NuMA protein was be carried out, under subcontract, at the Lelièvre laboratory at Purdue University. Image collection, the development of novel image analysis techniques and the image analysis has be performed at our facility at LBNL.

By using model-based algorithms to investigate the changes in NuMA distribution, we hope to identify patterns within the supramolecular structure of the cell nucleus that are linked to the development of breast cancer.

Significant progress has been made in the last year.

1) The Knowles lab has been fortunate with the acquisition of a Coherent Enterprise ultra-violet (UV) laser for our Zeiss 410 confocal microscope and a Sun Microsystems Blade2000 Workstation. Both were provided by other funding sources. These acquisitions have increased our imaging and image analysis capability so significantly, that we have reacquire our entire NuMA image database. The UV excitation has allowed the use of dapi for total DNA staining, instead of TroPro3 which we previously used. Dapi emission has greater spectrally isolation than that of TroPro3 from the emission spectrum of our Texas-Red anti-NuMA antibodies. This has allowed us to collect the full Texas-Red spectrum which results in NuMA images with increased signal to noise ratio. It has also meant that the Purdue lab can now visually qualify the NuMA staining before the biology is shipped to LBNL. Previously the spectral overlap of TroPro3 and Texas-Red prevented the Lelièvre Lab from clearly seeing the NuMA distribution. Further, because dapi binds predominantly to chromatin, its use has given us new insights into the role chromatin packing plays in NuMA organization. The new computer has 4 times the processing power (duel 1 gigahertz processors) and 8 times the memory capacity (4 giggabytes of memory) of the previous computer. This has allowed us to analyze NuMA images with twice the optical resolving power than previously possible. A total of 53 slides containing HMECs of different phenotype were cultured, fluorescently labeled and delivered to the Knowles Lab by the Lelièvre Lab. Each of the chamber slide has 4 separate wells in which different cell phenotypes can be cultured. Additionally, 6 slides were delivered of frozen human mammary sections, 2 slides of normal tissue and 4 slides of malignant tissue. The Knowles Lab has worked very closely with the Lelièvre Lab to ensure the biology has been correctly mounted for high resolution imaging. Information about the slides received and the image analysis results and the project in general are online at: **http://dwknowles.lbl.gov/numa_project/**

2) Although we are primarily interested in the organization of NuMA at early growth stages, we have extended our studies by collecting images of NuMA organization after the cells have been cultured for between 10 to 12 days. Previously we had only studied proliferating cells at 4 to 5 days of culture. After 10 days of culture, nonmalignant cells have differentiated into well organized acini and malignant cells have proliferated into large unorganized clusters. Analysis of these images has altered our initial hypothesis about the way NuMA organizes in nonmalignant cells. Our greater understanding has been key in the further develop of our image analysis techniques. For example, we now understand that it is not the size of NuMA foci, as we previously thought, but the amount of aggregated NuMA in the foci and their sub nuclear organization that sets proliferating and differentiated nonmalignant cells and proliferating malignant cells apart (See below).

3) Also, thanks to the Lelièvre Lab, we started collecting images of NuMA organization in both normal and malignant human mammary tissue.

4) However, probably the most important development this last year has been a realization that our CV analysis is inadequate for quantifying the types of image features that sets cells of different phenotypes apart. We developed the CV analysis to be sensitive to the size of features within an image (Figure 1.) and had previously theoretically demonstrated that the CV analysis was extremely sensitive to the feature size when the features were all approximately the same size, mono-disperse (Figure 2.).

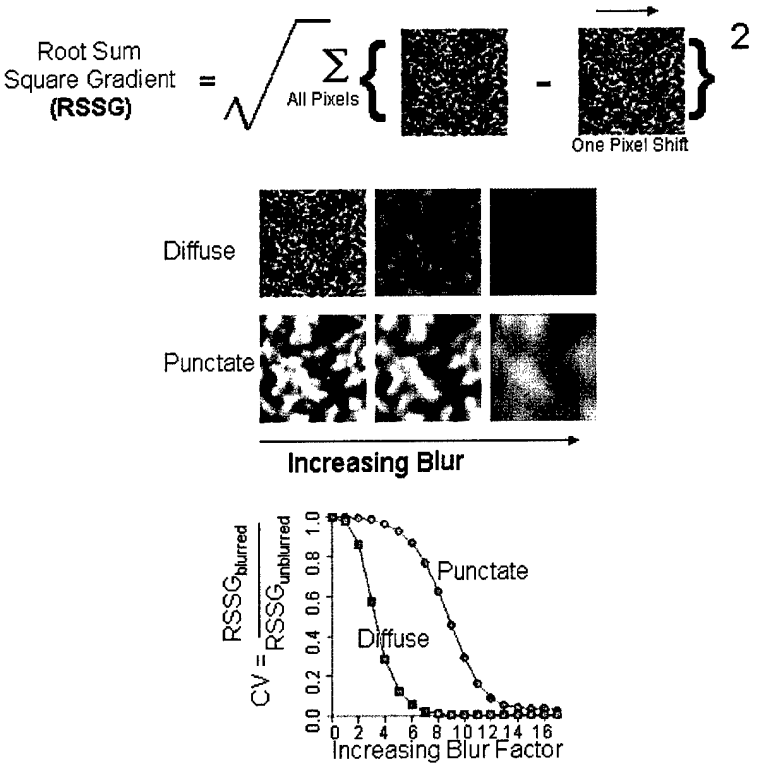

Figure 1: The Knowles Lab has developed an analysis called CV to quantify the size of punctate image features within each nuclear volume. For foci to exist, neighboring image points must have brightness values which correlate over the size of the foci. Conversely, diffuse staining results in rapid and unrelated brightness value variation. The total amount of brightness variation is thus inversely related to the average brightness correlation length which in turn is a measure of the foci size. Total brightness variation, called the root sum square gradient (RSSG), was calculated for the entire image as the root sum square of the all brightness variations along a given image direction (Fig. 1 top). To normalize this for image size, brightness, contrast and background brightness, the RSSG was calculated on the same image after it was blurred, mathematically, with a pseudo-Gaussian filter (Fig. 1 middle). The blurred image not only provided the means for normalization but also defined the brightness-correlation length over which the algorithm was sensitive. Dividing the blurred RSSG (RSSGblurred) with the unblurred RSSG (RSSGunblurred) produced a value from 0 to 1, termed the contrast variation (CV=RSSGblurred/RSSGunblurred) which is a measure of foci size (Fig. 1 bottom graph).

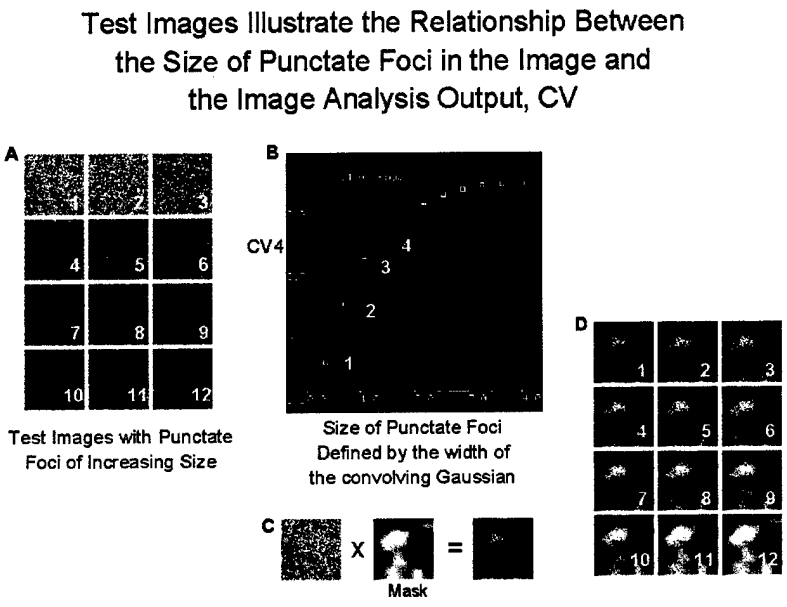

Figure 2. To determine the sensitivity of the image analysis algorithm to the size of foci, sets of well characterized test images of increasing punctate foci size were analyzed. The test images (Figures 2A1 - 2A12) were constructed by convolving a diffuse image with a Gaussian of increasing width. CV at blur factor 4 (CV4) was calculated and plotted against foci size for each image (Figure 2B). CV4 produced the largest increase over the punctate foci size of these images. CV2 would have saturated and CV8 would have not increased significantly. The results were unchanged if the diffuse image was first multiplied by a random background mask (Figure 2C) before being convolved with the Gaussian of increasing width (Figure 2D1 to 2D12).

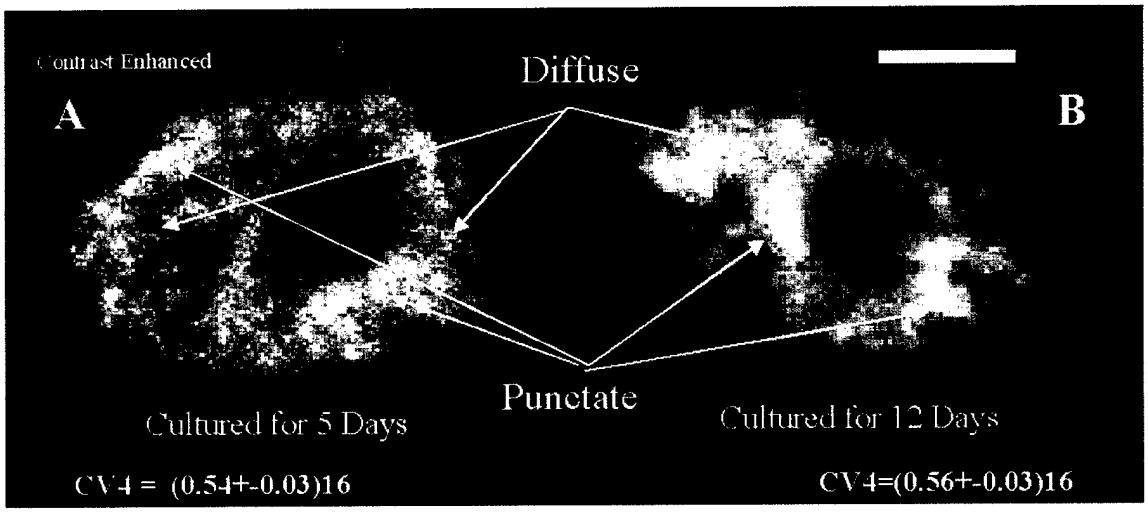

Figure 3: Nuclear Mitotic Apparatus Protein (NuMA) organizes into bright foci as cultured human mammary epithelial cells (HMECs) organize into tissue-like structures, acini. Two fluorescence micrographs of Texas-Red labeled anti-NuMA antibodies are shown for two nonmalignant nuclei cultured for 5 days (Figure 3A) and 12 days (Figure 3B). The CV analysis on 16 different 3D images of cells cultured for these periods are also given. After 5 days in culture the average CV4 was (0.54+-0.03) and after 12 days the CV4 was (0.56+-0.03). The CV analysis is clearly telling us that the size of foci is similar in these images even though there are clear visual differences between them.

The new images of NuMA are of far greater quality than previously collected and visual inspection indeed revealed the differences previously reported in nonmalignant cells (Lelièvre et

al., 1998) (Figure 3.). However, when we applied the CV analysis to images of NuMA in nonmalignant cells cultured for 5 days and 12 days, the results suggested it was not sensitive to the organizational differences in NuMA in our new data (Figure 3.). The CV analysis was clearly telling us that it was not the size of NuMA foci that was important. However, without knowing which image features were of importance it was difficult to develop the model-based image analysis techniques required. In fact it would have been impossible without the images of NuMA organization at later growth stages (Figure 3B) which certainly held the key. These images showed that it was not so much the size of the foci but their brightness or prominence and their subnuclear organization that was important. With this new insight, a new image analysis technique was created. It was derived to mimic Dr. Knowles' theory of the way the visual cortex perceives local bright features in a scene, even when the features are subtle and not well defined. Individual nuclei in the NuMA image (Figure 4A) are segmented by a mask created from the dapi image (Figure 4B). The NuMA image is then manipulated to create an image, which we have termed the local bright feature (lbf), which provides a new view of the NuMA organization (Figure 4E). This image can be simple normalized, by calculating the probability distribution of its brightness values (Figure 4F) and we have plotted these on a log10 scale (Figure 4G) to more clearly reveal the entire distribution. This normalization allows different images to be quantitatively compared.

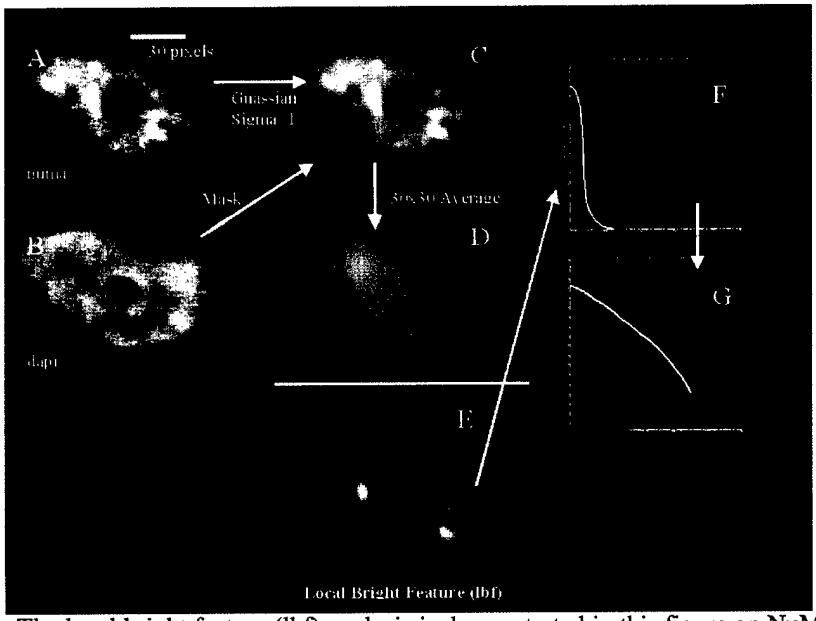

Figure 4. The local bright feature (lbf) analysis is demonstrated in this figure on NuMA staining from a single nuclei. Primary data are collected as fluorescence images of Texas-Red anti-NuMA antibodies (A) and dapi counterstained DNA (B). The dapi image is used to create a segmentation mask [Ortiz de Solorzano et al 1999] which delineate the boundary of individual nuclei and which is applied to the NuMA image. Before the mask is applied, the NuMA image is first convolved with a narrow Gaussian filter (sigma=1), designed to remove shot noise or detector noise from the image (C). The local average for every point in this image is then determined using a 30x30 pixel kernel (D). Note the scale bar in A is 5 microns or 30 pixels wide. The lbf image is then determined as the positive values that result after the local average image D is subtracted from the NuMA image C. Note that the lbf image is the positive deviation of pixel values from their local average. Normalizing the histogram of these pixel values creates the probability distribution (F) which is the normalizing factor that allows different images to be quantitatively compared. Plotting the resulting probability distribution on a log10 scale clearly reveals the entire distribution. Note: the information in the lbf image is brightness information and as such is only a relative measure. Like other techniques that rely on image brightness, the lbf image is dependent on the amplification or the sensitivity of the imaging device, and this intern depends on the effeciency and amount of fluorescence labeling, and the relative fluorophor quantum yeild.

Results of this new analysis are presented in the following figures. Each contains (1) a representative lbf image, which has been collapsed in the Z direction for 2D presentation, and (2) overlaid plots of the probability distribution, one for each lbf image in the set collected for that phenotype. Since this technique has been recently developed, and to our knowledge completely novel, we are yet to work out the best way to interpret and present the results. One aspect of this currently being working on, but presently undecided, is how best to turn the results from the probability distribution into a single quantitative metric. Here we simply report the trends of the distributions but point out that the average probability over the image set for finding the pixel values 50 and 100 in the lbf image are excellent markers of discrimination for the following results.

The new analysis indeed reveals quantitative differences in NuMA organization, visually obvious, between early growth and late growth nonmalignant cells. Figures 5, 6 and 7 report results for nonmalignant HMECs cultured for 3 days, 5 days and 12 days respectively. The probability distributions clearly show trends towards increased pixel values as the number of days in cell culture increases. This demonstrates that the amount of NuMA aggregated in foci is increasing. After 3 days of culture, nonmalignant cells are proliferating. Figure 5 shows that although there are definite NuMA foci, that pixel values in the lbf image were all low and fell below 100 except for one image, where the probability distribution extended above 100 (Figure 5C). Examination of that image showed that the cause was a single mitotic nuclei in which the NuMA had aggregated at the spindle poles (Figure 5B). We have pointed this out because it demonstrates the sensitivity of the technique to rare events. After 5 days of culture, nonmalignant cells start to organize into clusters of cells (Figure 6B) which will eventually growth arrest, differentiate and form acini. Thus, at day 5 it is possible that both proliferating and growth arrested cells are present. Notice that the lbf image (Figure 6B) shows there is clear organization of aggregated NuMA at the perimeter on the nuclei which was not present in cells after 3 days of culture (Figure 5B). The probability distribution (Figure 6A) also shows a marked jump to include increased pixel values. For these images the average probability of pixel value 100 in the lbf image is between 10^{-5} and 10^{-6}. Pixel value 100 simply did not register in Figure 5. Note also, the probability of pixel value 50 has jumped an order of magnitude to 10^{-3}. After 12 days in culture, nonmalignant cells have growth arrested and formed tissue-like structures (Figure 7B). Between 20 to 30 cells form a single polarize layer which surround a hollow central luman. The lbf image (Figure 7B) clearly shows bright foci organized around the internal nucleoli and at the perimeter of the nucleus. The probability distribution (Figure 7A) shows another marked increase towards higher pixel values.

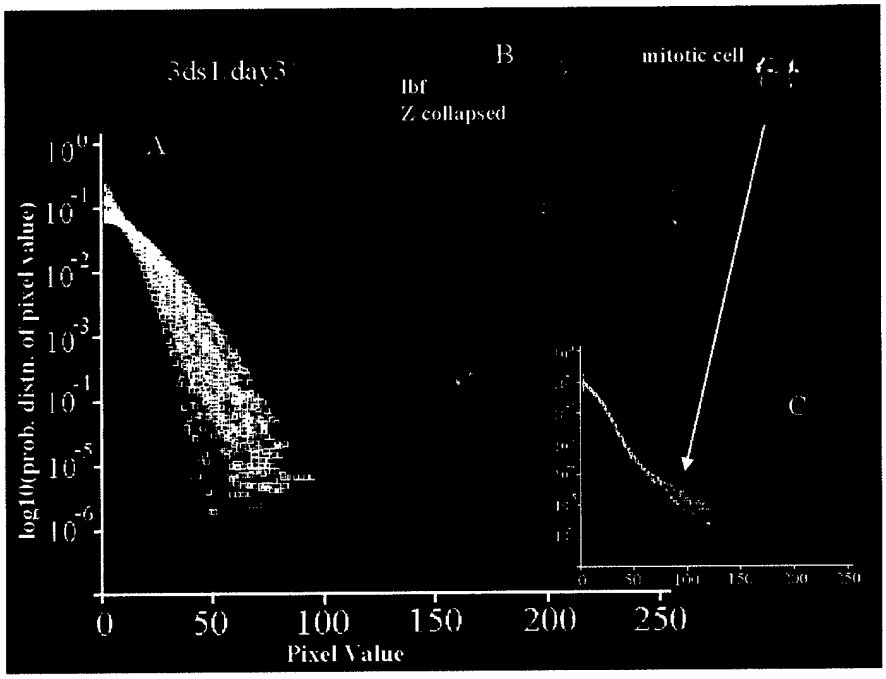

Figure 5. Nonmalignant HMECs cultured for 3 days. Panel A shows overlaid plots of the probability distribution of pixel values of 15 lbf images. Panel B shows a single lbf image collapsed in the Z direction for 2D display. The NuMA organization shown is representative in all but one nuclei which is in the mitotic phase. Panel C shows the effect of that single mitotic nuclei in which NuMA is highly aggregated at the spindle poles.

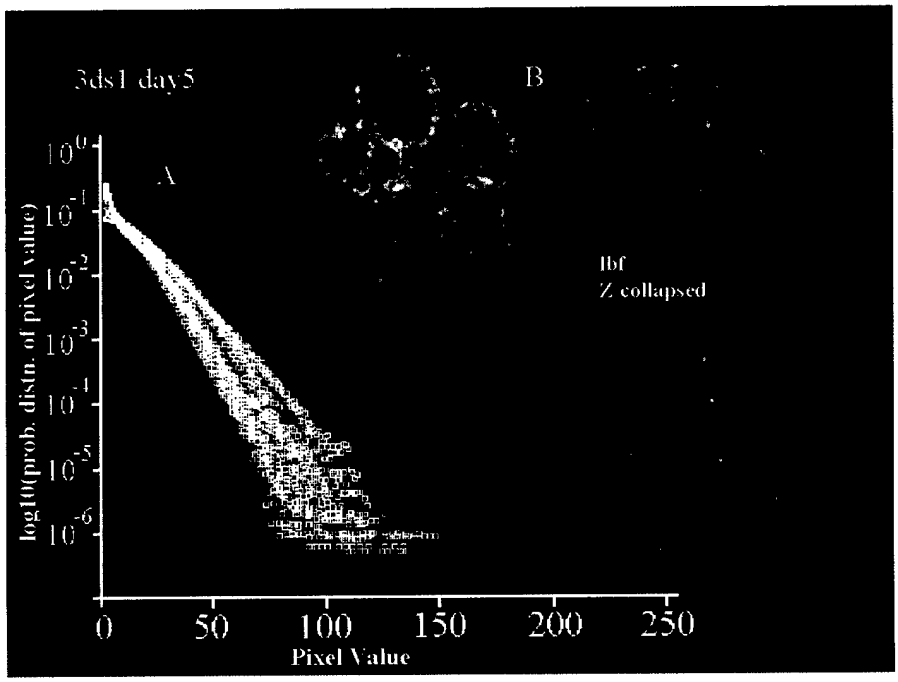

Figure 6. Nonmalignant HMECs cultured for 5 days. Panel A shows overlaid plots of the probability distribution of pixel values of 16 lbf images. Panel B shows 3 lbf images collapsed in the Z direction for 2D display. They show NuMA is organized at the perimeter of the nucleus.

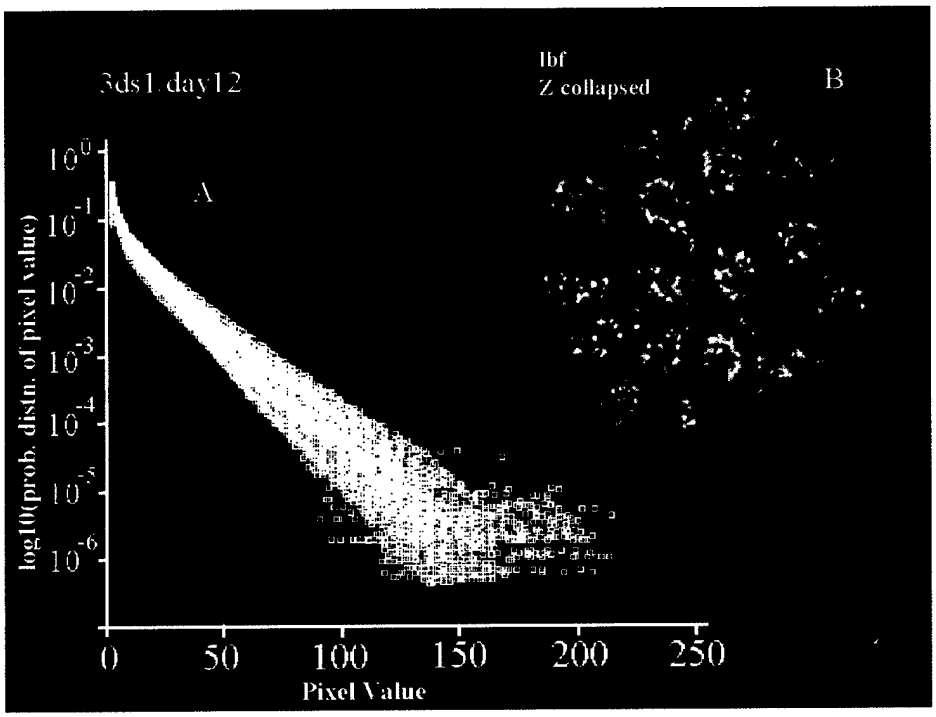

Figure 7. Nonmalignant HMECs cultured for 12 days. Panel A shows overlaid plots of the probability distribution of pixel values of 43 lbf images. Panel B shows an lbf image collapsed in the Z direction for 2D display. Notice that here the average probability of pixel value 100 in the lbf image is around 10^{-4}, nearly two orders of magnitude greater than that for cells cultured for 5 days in Figure 6.

All these results are very good news but how do they relate to the organization of NuMA in malignant cells and can the analysis discern proliferating malignant from proliferating nonmalignant cells? Figure 8 shows the results from all the malignant HMECs. Interestingly, there was no measurable difference in the organization of NuMA as the number of days in cell culture increased. This was not surprising because these cells do not differentiated into structures but grow into large unorganized clusters. The probability distributions from lbf images of these cells (Figure 8A) showed a marked decrease from differentiated nonmalignant cells (Figure 7A) but the curves were very similar to those produced from lbf images of nonmalignant cells at day 5 (Figure 6A). The analysis suggests there are foci of NuMA in malignant cell with about the same prominence of those in proliferating nonmalignant cells. However, the answer seems to lie in the organization of the foci. In the malignant cell there is no evidence of localized organization, in fact the foci of NuMA appear randomly distributed through out the nuclei (Figure 8B). This was certainly not the case for the proliferating nonmalignant cells (Figure 6B).

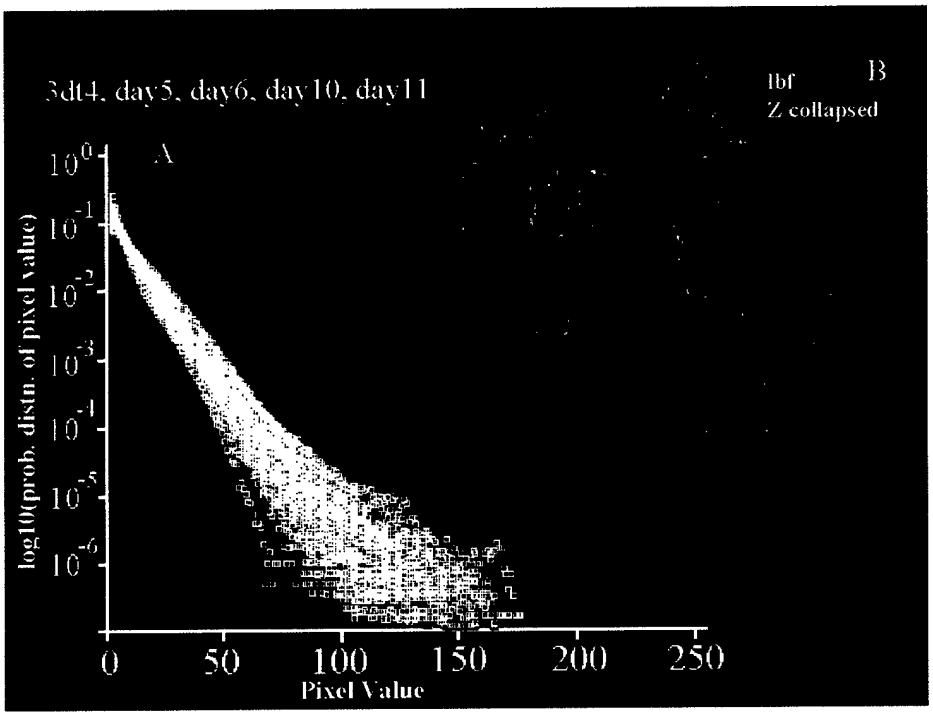

Figure 8. Malignant HMECs cultured for 5, 6, 10 and 11 days. Panel A shows overlaid plots of the probability distribution of pixel values of 30 lbf images. Panel B shows a representative lbf image collapsed in the Z direction for 2D display. This image suggests that foci of NuMA in these cell are organized randomly throughout the nuclei.

The final 2 figures, show results from our images of NuMA organization in normal and malignant frozen (20 micron thick) sections of human mammary tissue. Figure 9 shows results from 9 images of normal human tissue. The lbf image clearly shows many bright NuMA foci. The resulting probability distributions (Figure 9A) are indistinguishable from the results from differentiated nonmalignant cells (Figure 7A) indicating that indeed our nonmalignant model tissue system has a normal phenotype. The result is very pleasing. Figure 10 shows results from 25 lbf images from regions of the malignant tissue that look phenotypically abnormal, based on visual observations of the region images under low magnification (Figure 10D). Although the probability distributions are not very different from those in the normal case, we believe further analysis will reveal at least two distinct populations of cells in these cases, based on visual observations of their NuMA organization.

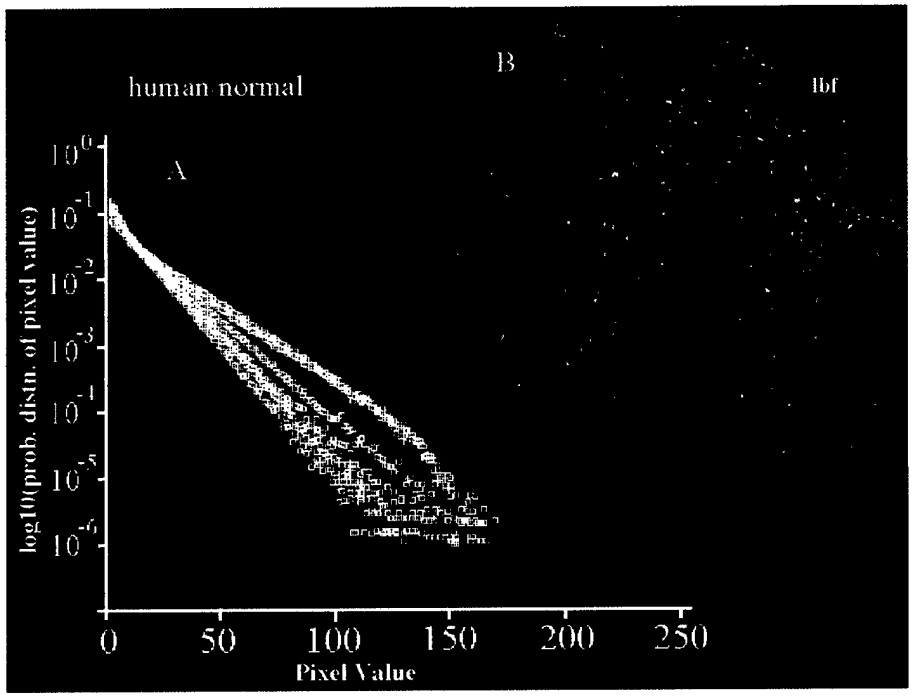

Figure 9. Normal human mammary tissue. Panel A shows overlaid plots of the probability distribution of pixel values of 9 lbf images. Panel B shows a representative lbf image collapsed in the Z direction for 2D display. The results are indistinguishable from those from differentiated nonmalignant cells (Figure 7A) indicating that indeed our nonmalignant model tissue system has a normal phenotype.

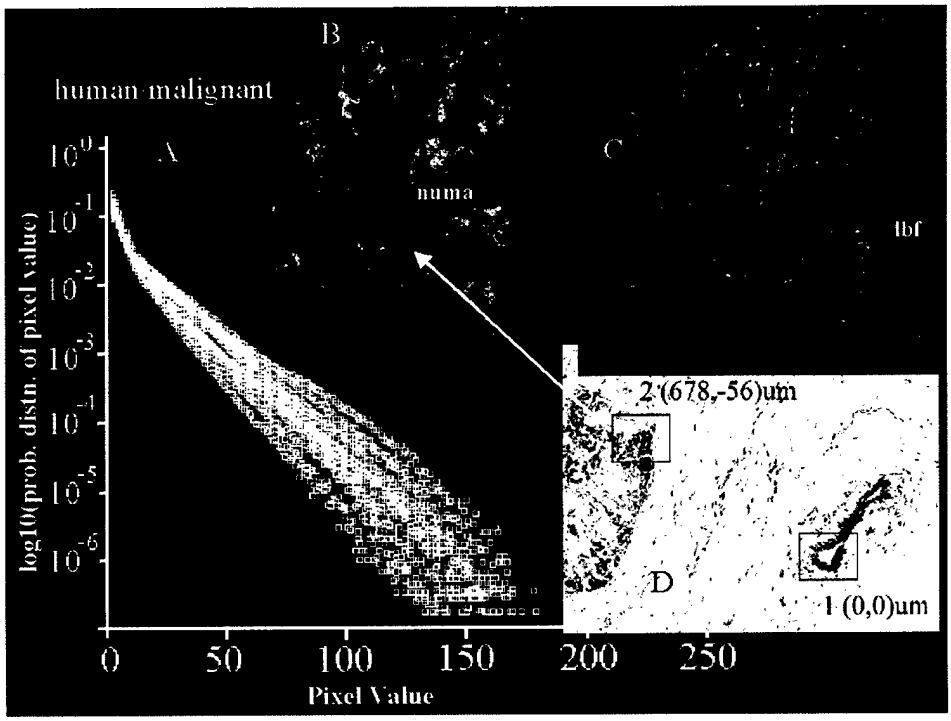

Figure 10. Malignant human mammary tissue. Panel A shows overlaid plots of the probability distribution of pixel values of 25 lbf images. Panel B shows the raw NuMA image and panel C the corresponding a lbf image, collapsed in the Z direction for 2D display. Panel D shows a low power gray scale inversion of the dapi image which reveals something about the phenotype of nuclei being imaged. Although the probability distributions are not very different from those in the normal case, we believe further analysis will reveal at least two distinct populations of cells in these cases, based on visual observations of their NuMA organization.

KEY RESEARCH ACCOMPLISHMENTS:

* Acquisition of UV laser for the confocal microscope and a new computer has allowed images of far greater quality to be acquired and analyzed. Because of this we have reacquired our entire NuMA image data base.

* We have extended our studies by collecting images of NuMA organization after the cells have been cultured for between 10 to 12 days. The images clearly show that NuMA aggregates into bright foci as the cell differentiate, as previously reported. Analysis of these images has altered our initial hypothesis about the way NuMA organizes and has been key in the further develop of our image analysis techniques.

* We have extended our studies of NuMA organization to normal and malignant human mammary tissue.

* We have realized that our previous CV analysis is not the right tool for quantifying our NuMA images.

* We have developed a new image analysis method based on our increased understanding of NuMA organization, which extracts the local bright features from an image.

* The new image analysis technique clearly shows that NuMA aggregates into foci in both proliferating nonmalignant and differentiated nonmalignant cell. Further, that in proliferating nonmalignant cells, NuMA foci organized on the outside of the central nucleolus and at the perimeter of the nucleus.

* The new analysis shows that NuMA foci are present in proliferating malignant cell but the foci have no specific organization. Rather they are distributed randomly throughout the nucleus.

* The new analysis does not quantitatively distinguish between the brightness or organization of NuMA foci in normal human tissue from those in differentiated nonmalignant cells. This is very pleasing because it supports the theory that our nonmalignant cultured model tissue system has normal phenotype.

* We believe that future refinements to our new analysis will reveal at least two population existing in our images of malignant human tissue.

REPORTABLE OUTCOMES:

David W. Knowles, Sophie A. Lelièvre, Carlos Ortiz de Solórzano, Stephen J. Lockett, Mina J. Bissell, Damir Sudar 2001 *Quantitative model-based image analysis of NuMA distribution links nuclear organization with cell phenotype* Microsc. Microanal. 7:578-579

CONCLUSIONS:

Our current results are very exciting because they demonstrate that, using model-based image analysis, we can distinguish between non-malignant and malignant cells that are both in an early growth proliferation stage. To our knowledge, there were no known markers or tools that permitted such a distinction before.

One essential feature of the image analysis not addressed in this report is the segmentation algorithm, which delineates nuclei in the 3D dapi images. In the past year the segmentation algorithm we have used has been completely automated and does a good job of segmenting all nuclei but the segmentation often results in clusters of multiple nuclei. Currently we are working on methods which will maintain as much segmentation automation as possible but result in independent segmentation of each nucleus. Although our current results clearly indicate differences in the subnuclear organization of NuMA, better nuclei segmentation will allow NuMA image analysis to be directed on a nucleus by nucleus bases. This will open the door in the near future for quantitative analysis of the organization of NuMA foci at subnuclear resolution. We believe this is the next very important step to be taken in this project.

REFERENCES:

Lelièvre SA, Weaver VM, Nickerson JA, Larabell CA, Bhaumik A, Petersen OW, Bissell MJ. 1998 *Tissue phenotype depends on reciprocal interactions between the extracellular matrix and the structural organization of the nucleus.* Proc Natl Acad Sci U S A. 95:14711-6

Ortiz de Solorzano C, Garcia Rodriguez E, Jones A, Pinkel D, Gray JW, Sudar D, Lockett SJ. 1999 *Segmentation of confocal microscope images of cell nuclei in thick tissue sections.* J Microsc. 193:212-26.

APPENDICES:

QUANTITATIVE MODEL-BASED IMAGE ANALYSIS OF NuMA DISTRIBUTION LINKS NUCLEAR ORGANIZATION WITH CELL PHENOTYPE

David W. Knowles, Sophie A. Lelièvre [+], Carlos Ortiz de Solórzano, Stephen J. Lockett [++], Mina J. Bissell, Damir Sudar

Life Sciences Division, Lawrence Berkeley National Laboratory, Berkeley, California 94720

[+] Department of Basic Medical Sciences, Purdue University, West Lafayette, IN 47907-1246

[++] SAIC-Frederick, MD 21702

The extracellular matrix (ECM) plays a critical role in directing cell behaviour and morphogenesis by regulating gene expression and nuclear organization. Using non-malignant (S1) human mammary epithelial cells (HMECs), it was previously shown that ECM-induced morphogenesis is accompanied by the redistribution of nuclear mitotic apparatus (NuMA) protein from a diffuse pattern in proliferating cells, to a multi-focal pattern as HMECs growth arrested and completed morphogenesis [1]. A process taking 10 to 14 days.

To further investigate the link between NuMA distribution and the growth stage of HMECs, we have investigated the distribution of NuMA in non-malignant S1 cells and their malignant, T4, counter-part using a novel model-based image analysis technique. This technique, based on a multi-scale Gaussian blur analysis (Figure 1), quantifies the size of punctate features in an image. Cells were cultured in the presence and absence of a reconstituted basement membrane (rBM) and imaged in 3D using confocal microscopy, for fluorescently labeled monoclonal antibodies to NuMA (fαNuMA) and fluorescently labeled total DNA. Nuclear segmentation [2], based on the DNA staining, allowed NuMA distribution analysis to be contained within the nuclei of individual cells.

fαNuMA distribution was clearly less punctate in non-malignant S1 cells in rBM culture at day 4 (proliferation) than at day 10, when these cells complete differentiation, as previously reported. Interestingly, the distribution of fαNuMA in malignant T4 cells, in rBM culture at day 4, was measurably less punctate than that in S1 cells at either time. This supports the phenotypic trait of T4 cells cultured in rBM which is their inability to differentiate. In the absence of rBM, non-malignant S1 cells are also unable to differentiate but proliferate in presence and growth arrest in absence of epithelial growth factor (EGF). Again, there was a clear measurable difference between fαNuMA distribution which was less punctate during proliferation and more punctate when these cells growth arrested. Interestingly, in the absence of rBM there was no measurable difference in fαNuMA distribution in proliferating S1 cells and their malignant counterpart which also possibly reflects the inability of either cell type to differentiate.

The ability to discern cell phenotype based on quantifyable molecular analysis, in this case the spatial distribution of a nuclear protein, has broad application in furthering fundamental understanding of biological processes.

[1] **Sophie A. Lelièvre**, et al **1989**
Tissue phenotype depends on reciprocal interactions between the extracellular matrix and the structural organization of the nucleus
PNAS 1998 95: 14711-14716.

[2] **Ortiz de Solórzano C.**,et al **1999**
Segmentation of Confocal Microscope Images of Cell Nuclei in Thick Tissue Sections
Journal of Microscopy, 193(3):212-226

Microsc. Microanal. 7 (Suppl 2: Proceedings)

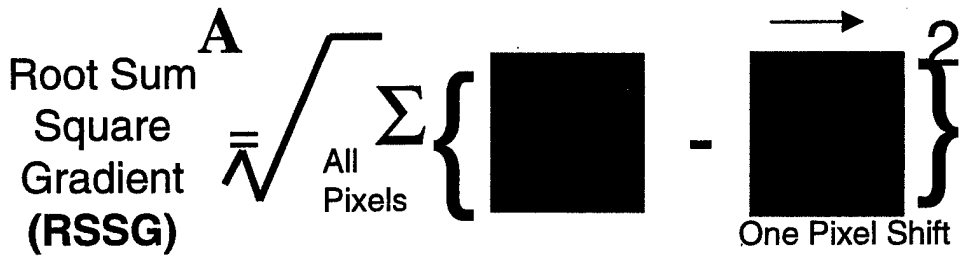

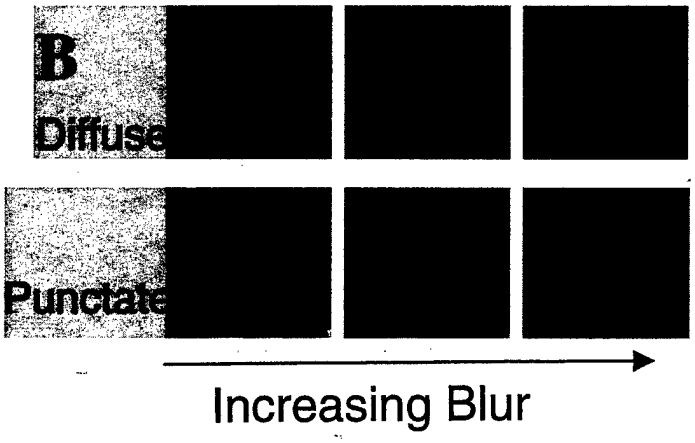

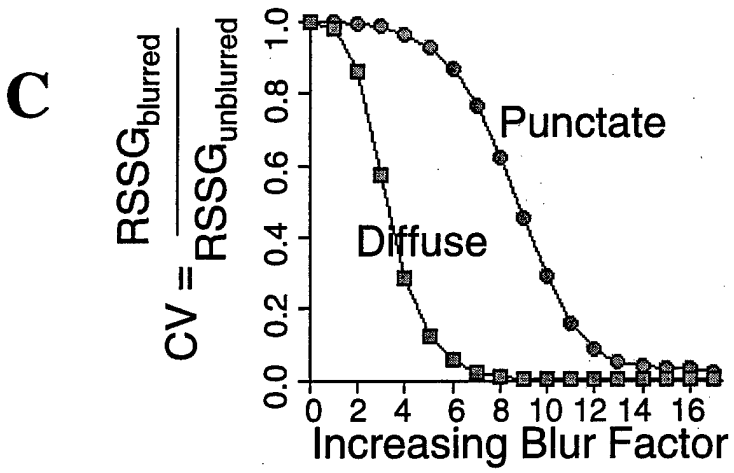

As a measure of the size of punctate features in an image, we use the root sum square gradient (RSSG), defined as the root sum square of the difference in neighouring voxel values, along a given direction, throughout the image (**Figure 1A**). To normalize this for image size, brightness, contrast and background brightness, the RSSG is calculated on the same image after it has been blurred, mathematically, with an Gaussian (like) filter (**Figure 1B**). Increasing the Gaussian blur factor in this step increases the range of foci sizes to which the analysis is sensitive. Dividing the blurred RSSG (RSSGblurred) with the unblurred RSSG (RSSGunblurred) produces a value from 0 to 1 which we have termed the contrast variation (CV= RSSGblurred/RSSGunblurred) (**Figure 1C**) which relates to the size of punctate features in the image.